

Design of a High Altitude Balloon Drop Test for SPORE (Small Probes for Orbital Return of Experiments)

Jessica Juneau

School of Aerospace Engineering

AE 8900

Spring/2012

Advisor: Prof. David A. Spencer

Signature: _____

Date: _____

Grade: _____

Design of a High Altitude Balloon Drop Test for SPORE (Small Probes for Orbital Return of Experiments)

Jessica Juneau Clark¹ and David A. Spencer²
Georgia Institute of Technology, Atlanta, GA, 91206

The Small Probes for Orbital Return of Experiments (SPORE) flight system is designed to perform atmospheric entry, descent and landing (EDL) in order to return small payloads from an Earth orbit to the ground for recovery and laboratory analysis. A high altitude balloon drop test of a nearly identical re-entry probe, weighing 10.51 kg is described. In order to test the parachute deployment system and canopy performance at flight-like dynamic pressures and Mach numbers, a drop altitude of 32.8km from a 0.11 mcm balloon was determined to be sufficient, based on a float altitude trade study. A Monte Carlo analysis of the drop test trajectory was performed to characterize variability of chute deployment conditions and landing ellipse size. A description of launch and ground operations is included, as well as a preliminary probe and gondola design. Finally, an overview of similar historical stratospheric balloon drop test programs is provided.

¹ Masters Student, Aerospace Engineering Dept., 225 North Ave, Atlanta, GA 30332.

² Professor (Research Advisor), Aerospace Engineering Dept., 225 North Ave, Atlanta, GA 30332.

Nomenclature

$C_{D_o}S_o$	=	Parachute nominal drag area (m ²)
<i>CSBF</i>	=	Columbia Scientific Balloon Facility
C_X	=	Parachute opening load factor (unit-less)
D	=	Drag force
D_o	=	Parachute nominal diameter (used for reference area in C_{D_o})
<i>DOF</i>	=	Degree Of Freedom
<i>EDL</i>	=	Entry, Descent, and Landing
F_{eject}	=	Mortar ejection force
F_P	=	Parachute force (drag on entry vehicle due to parachute)
F_S	=	Parachute snatch force
<i>FPA</i> , γ	=	Flight Path Angle (negative below horizon)
γ_o	=	Initial flight path angle
g	=	Gravitational acceleration
<i>GTO</i>	=	Geosynchronous Transfer Orbit
h, h_o	=	Altitude, initial altitude
<i>HAB</i>	=	High Altitude Balloon
<i>HASI</i>	=	Huygens Atmospheric Structure Instrument
<i>ISS</i>	=	International Space Station
l_{lines}	=	Length of bridle, riser, and suspension lines of parachute
<i>LEO</i>	=	Low-Earth Orbit
M	=	Mach number
m, m_o	=	Vehicle mass, initial vehicle mass
<i>mcm</i>	=	Million cubic meter (1×10^6 m ³)
<i>NSC</i>	=	Near Space Corporation
n	=	Canopy fill constant (specific to canopy type)
<i>PEPP</i>	=	Planetary Entry Parachute Program (Viking)
<i>POST</i>	=	Program to Optimize Simulated Trajectories
ϕ, ϕ_o	=	Latitude, initial latitude (deg N)
ψ, ψ_o	=	Heading angle, initial heading angle
q	=	Dynamic pressure (Pa)
r	=	Radius from center of Earth to vehicle
<i>SPORE</i>	=	Small Probes for Orbital Return of Experiments
<i>STTR</i>	=	Small business Technology TRansfer program (NASA)
t	=	Time
t_d	=	Time of parachute mortar fire (after separation from gondola)
t_{FI}	=	Time of parachute full inflation
t_{LS}	=	Time of parachute line stretch
θ, θ_o	=	Longitude, initial longitude (deg E)
V, V_o	=	Earth-relative velocity, initial Earth-relative velocity
V_{eject}	=	Relative parachute ejection velocity (from mortar fire)
V_{LS}	=	Velocity of vehicle at line stretch

Table of Contents

Design of a High Altitude Balloon Drop Test for SPORE (Small Probes for Orbital Return of Experiments) 1
Nomenclature 3
Table of Contents 4
I. SPORE Overview 5
II. Introduction: High Altitude Balloon Drop Test 5
III. Historical Balloon Drop Programs 6
 A. Test Objectives 6
 B. Test Setup 6
 C. Gondola and Probe Design 7
 D. Instrumentation 7
IV. HAB Launch Providers 7
 A. Near Space Corporation 7
 B. Columbia Scientific Balloon Facility 8
V. Test Configuration Trade Study 9
 A. 3-DOF Trajectory Simulation 9
 B. Parachute Model 9
 C. Aeroshell Drag Model 10
 D. Atmospheric Winds Model 11
 E. Defining the SPORE Parachute Deployment Conditions 12
 F. Defining the Drop Test Conditions 13
VI. Monte Carlo Analysis 16
 A. Uncertainty Characterization 16
 B. Results 17
VII. Test Vehicle Design 20
 A. Entry Capsule Design 20
 B. Gondola Design 22
VIII. Ground and Launch Operations 23
 A. Pre-Flight Activities 23
 B. Launch and Flight Activities 24
IX. Conclusions 25
Appendix A: Historical Balloon Drop Tests 26
Acknowledgments 33
References 34

I. SPORE Overview

THE Small Probes for Orbital Return of Experiments (SPORE) flight system architecture provides a scalable, modular approach to the return and recovery of multi-purpose probes from orbit. Capable of accommodating payload volumes ranging from the CubeSat 1-unit (1U) dimensions of 10x10x10 cm to 2U and 4U payloads, SPORE is targeted to carry flight experiments related to thermal protection system (TPS) performance validation, biological science, and materials science missions. SPORE is also designed to accommodate the return of small payloads from the International Space Station (ISS).

The Entry, Descent, and Landing phase for SPORE is designed to meet thermal control and g-level requirements to maintain payload health and safety. Because the desired on-orbit environment for different payloads varies dramatically, the SPORE architecture is designed to accommodate re-entry from orbits ranging from low-Earth orbit (including ISS return) and GTO. Landing sites at the Utah Test & Training Range and the Woomera Test Range in South Australia are targeted.

The EDL sequence begins when the SPORE entry vehicle is deployed from its service module following a de-orbit maneuver that targets a zero degree initial angle of attack, ballistic reentry trajectory. Peak heating and maximum deceleration are experienced during the hypersonic regime, and following the transition to subsonic flight, the cross parachute is ejected using a mortar. No jettison of the heatshield is required, as the payload is thermally isolated from the heatshield soak-back. The vehicle approaches terminal velocity on the parachute prior to touchdown, with touchdown velocities varying based upon the vehicle configuration. A UHF beacon signal will be transmitted throughout EDL to aid in the recovery process. Recovery is required to occur within two hours of touchdown.

II. Introduction: High Altitude Balloon Drop Test

As part of the NASA STTR Phase II effort, it is desired to increase the SPORE flight system TRL through various tasks. Of these tasks, a high altitude drop test of the entry system would provide a means of verifying flight system functionality in a near flight-like environment. High altitude balloons (HABs) provide a relatively low-cost, quick-response method for delivering the entry system to a desired altitude and releasing it, in order to test system functionality during atmospheric descent and landing. Most HAB tests can be flight-ready in as little as 6 months, and can be launched from a variety of locations because of their mobile launch platform. High altitude balloons have been used for similar drop tests on a number of NASA and ESA missions, as is detailed in Section II.

A typical test setup involves transporting the flight payload (for SPORE: the gondola and entry vehicle) to the launch pad via a crane, assembling the flight train, inflating the tethered balloon, releasing the balloon and then the payload. After the flight train reaches the desired float altitude, gondola release can be triggered from ground command, at which point the entry vehicle separates and begins to free-fall. Parachute deployment occurs autonomously, and the entry vehicle, gondola, and deflated balloon are all recovered on the ground. A more detailed description of launch and ground operations can be found in Section VIII.

For the SPORE HAB drop test, the primary objectives would be the following:

- Verify entire entry system functionality, thereby increasing the entry system TRL. This includes the communications system, command and data handling system, electrical power system, and parachute deployment system.
- Verify parachute canopy integrity at flight-like dynamic pressures and Mach numbers
- Investigate entry vehicle stability at subsonic conditions
- Gain experience with mission operations planning, hardware testing and integration, and pre- and post-flight procedures

The following sections document the initial work that has been done in designing the SPORE high altitude balloon test. This work includes surveying similar historical balloon drop programs, investigating potential HAB launch providers, and performing trade studies and Monte Carlo analyses to determine the optimal test conditions and to characterize the influence of variability on test outcomes. In addition, a preliminary description of the entry vehicle and gondola design is discussed, as well as launch and ground operations setups.

III. Historical Balloon Drop Programs

High altitude balloon drop tests have long been used by NASA, ESA, and other aerospace organizations as a means of testing system functionality in a flight-like environment for relatively low cost and complexity. In order to provide a historical perspective in designing the SPORE drop test, a thorough study of similar historical balloon drop test programs was performed. Many of these programs had test objectives and flight conditions that were very similar to the SPORE drop test, and were conducted as a part of large NASA, ESA, and JAXA missions. The missions whose supporting drop tests were investigated include Galileo, Cassini-Huygens, Haybusa, Stardust, Viking, and NASA Mars subsonic parachute studies. Below is a summary of the test programs that are most applicable and useful for the SPORE drop test design. A more detailed description of these tests can be found in the References Section and the table listed in Appendix A.

A. Test Objectives

Most of the drop test programs investigated had test objectives that were similar to those of the SPORE drop test. All of them sought to, in some way, demonstrate proper parachute deployment at conditions that were as flight-like as possible. The Mars subsonic parachute tests, conducted by Mitcheltree et al.¹² in 2004 were part of an effort to develop a new parachute system for Mars exploration, and so the parachute was the primary drop test payload, whereas the larger mission tests were purposed for testing the entire entry system functionality. Both the Hayabusa MUSES-C and the Huygens probe drop tests had objectives for characterizing vehicle transonic aerodynamics and probe stability.^{9,7} Observing the re-entry probe dynamics in a flight-like spin was also an objective of the Huygens probe drop tests.⁹ After the initial Huygens probe drop test, an additional test was conducted to test spare sensors of the HASI (Huygens Atmospheric Structure Instrument) in dynamic conditions and to test their trajectory reconstruction algorithms.^{3,4} In most of these drop test programs, the test objectives were fully met, with some exceptions where technical failures on the customer's part occurred or where the ideal flight conditions were too extreme for a low-altitude, Earth drop test.

B. Test Setup

The target float altitudes for the various drop test programs ranged from 29 km (Galileo) to 40 km (Viking PEPP), except for the 3.62 km Stardust drop test to test the basic entry system functionality.¹⁸ Balloon volumes, ranging from 0.03 mcm (Hayabusa) to 0.74 mcm or million cubic meter (Viking PEPP) were used to lift suspended masses between 500 and 1500 kg.

The ascent train, or vertical chain of hardware lifted in a balloon test, can be varied from test to test, but has the same basic structure. A typical ascent train features the payload, attached to or internal to a support gondola. Above the gondola is a mechanical/electrical gondola release mechanism that is typically signaled to release via ground command. Most tests require a safety or emergency parachute above the gondola release mechanism in the event of balloon failure or for use as a means of recovering the gondola. Above the safety chute is the terminate release mechanism, which can be used to recover the support gondola (and payload, if a free fall is not desired) under the safety chute. At the top of the ascent train is the balloon, which is typically deflated upon gondola release and recovered on the ground as well. The basic ascent train can be modified, of course, to accommodate drop test needs or requirements. For the initial Huygens system drop test an auxiliary balloon was used in addition to the main Type 402 Z balloon⁷, and for the later HASI test, a separate Telemetry Module (TM) was added 2.6 m above the probe and below the parachute via a heavy bifilar line (See Figure 25 in Appendix A).^{3,4} The TM contained all instruments and supporting devices to perform probe release.^{3,4} Other variations of the ascent train utilized the gondola release event to static-line deploy the drogue or main chute, as with the Stardust drop test, Huygens HASI test, the Mars subsonic test program.^{18,12,3,4}

Most of the historic drop tests featured a two-stage parachute system (drogue and main). For the Mars subsonic parachute tests, the drogue was static-line deployed after gondola release, and the time-triggered main chute was deployed with pyro cutters.¹² The Galileo probe drop tests featured a pilot chute, followed by aft heatshield removal, and then the main chute deployment. After main chute deployment, the descent module was separated from the deceleration module, as would occur during the probe's actual mission (See Figure 23 for probe design and Figure 24 for deployment sequence).^{10,16} The Stardust systems drop test utilized the gondola separation event for static deployment of the drogue, followed by a computer-initiated main chute deployment.¹⁸ The Huygens probe utilized a three-stage parachute system, with a pilot chute deployed at Mach 1.5, a main chute for heatshield separation, and then a stabilizer chute for the remainder of atmospheric descent. All of the Huygens drop test separation events were based on majority voting.⁹ For the Huygens HASI test, a single, static-line deployed parachute was used, that was

linked to the balloon via a connector pyro cable and fired via ground command. The parachute was static-line deployed, and a ballast on the TM was also jettisoned via ground command^{3,4} Both of the Hayabusa drop tests also featured a single, toroidally packed parachute (one of which was 60% reefed), that were pulled out by the parachute cover and jettisoned using pyro pushers (See Figure 22).⁷

C. Gondola and Probe Design

The purpose of the gondola is to carry all support equipment for the balloon payload (be it a re-entry probe or scientific samples). It also serves as a mechanical and electrical interface between the payload and the balloon. For the Mars subsonic parachute tests, the gondola also served as the aerodynamic vehicle for the parachute system, and was released with the payload. It featured a truss structure, a faceted aerodynamic fairing, a structural base with instrumentation, and a crushable cardboard honeycomb on the nose to reduce the loading upon ground impact (See Figure 29).¹² The gondola for the Huygens probe drop test had bracket interfaces between the probe and gondola for pyro separation, umbilical separation by a lanyard, and also featured spin vanes to generate spin rates similar to those on the actual Huygens mission (See Figure 28).⁹ For the HASI experiment, the gondola was also equipped with spin vanes, and even carried lead bricks as a mass ballast (See Figure 26).³

For a majority of the drop test programs investigated, the payload was a geometrically similar (sometimes identical) mock-up of the actual re-entry probe. The probe for the Huygens drop test was a full-scale model of the actual entry vehicle, with flight-like hardware, as was the probe for the HASI experiment, with an additional ring supporting a double-plate platform, a bottom front cone, and an upper cover (See Figure 26). For the Galileo probe drop test, a 376 kg ballast was added to the nose of the probe, increasing the vehicle's ballistic coefficient, so that flight-like dynamic pressures could be achieved (Figure 23 shows Galileo probe design).¹⁰ The Hayabusa MUSES-C drop test probe featured an additional antenna mounted to the forward heat shield for communication with the ground, as shown in Figure 20.

D. Instrumentation

In terms of probe and gondola instrumentation, all of the historical missions carried some form of the following: primary batteries (with Power Distribution Unit), telecommunications equipment, on-board cameras, accelerometers, pressure transducers (stagnation and internal), thermal control equipment, rate gyros, pyrotechnic devices for separation events, and data acquisition and storage equipment. Detailed descriptions of the instrumentation used on each of the historical drop tests can be found in the table in Appendix A. For primary batteries, a range of types were used including Lithium-ion (Mars subsonic chute testing, sized for 10 hour duration¹²), NiCd rechargeable batteries (Huygens probe, Hayabusa MUSES-C), and Ni-MH (for HASI experiment, sized for 8 hour duration).³ Most telecommunication systems featured ground-to-gondola uplink and downlink, but the Huygens probe featured a L-band gondola-to-ground link, an S-band probe-to-gondola link, and an S-band probe-to-ground link for data backup, as diagramed in Figure 27. Most of the missions carried CCD or film cameras for monitoring parachute deployment and separation events. The Mars subsonic parachute test carried 2 up-looking mini-digital-video camcorders, 1 up-looking camera connected to telecoms for ground storage, an additional down-looking camera, 1 chase plane camera, and one ground telescope camera.¹² For altitude (and latitude/longitude) knowledge, some drop test probes carried on-board GPS's (Mars subsonic chute test, HASI test, and Huygens probe drop test). The Huygens probe drop test also used differential GPS between the probe and gondola.⁹ For the Hayabusa drop tests, the altitude was estimated using pressure transducer data and camera data. Most of the drop tests carried 1-axis or 3-axis accelerometers, and 2-axis rate sensors. The Mars subsonic chute test also carried a Northrup Grumman LN-200 IMU, with 3-axis rate gyros and 3-axis accelerometers.¹²

Information regarding the testing objectives, test setups, and probe/gondola instrumentation for similar historical missions provided invaluable references used to aid in the design of the SPORE drop test.

IV. HAB Launch Providers

Two US-based high altitude balloon launch providers were investigated as potential launch providers for the SPORE drop test: Near Space Corporation and NASA's Columbia Scientific Balloon Facility.

A. Near Space Corporation

Near Space Corporation (NSC) is a commercial corporation based in Tillamook, Oregon that has the facilities and capabilities to support high altitude balloon, airship, and UAV flight operations. Since its founding, NSC has conducted and overseen over 160 stratospheric balloon flights. It boasts facilities and equipment that include

multiple remote and established launch sites, an altitude chamber, a material testing lab, tracking aircraft, a self-contained mobile operations trailer, and specialized launch vehicles and equipment.¹⁴ The high altitude balloon equipment available at NSC can carry suspended masses up to 1360 kg to altitudes of approximately 40 km (well within the needs of the SPORE drop test). The staff at NSC also provides support for mission planning, FAA coordination, payload integration and check-out, balloon flight operations, mission control and telemetry, airspace deconfliction via tracking aircraft, payload recovery, and flight documentation.¹⁴

Their stratospheric balloon platform that is the most relevant to the SPORE drop test is their Small Balloon System (SBS). It is a traditional balloon platform and parachute recovery system that can lift payloads of up to 10kg to 35 km. While the SPORE drop test vehicle mass is likely to be slightly larger than 10 kg, they do offer non-standard options allowing for larger payload masses, higher altitudes, or remote launch sites. All of the SBS standard launch operations are conducted out of NSC’s Tillamook Balloon Facility in Oregon.¹⁴ More information regarding NSC’s flight procedures can be found on their website: www.nsc.aero.

NSC is also included as a high altitude balloon launch provider for NASA’s Announcement of Flight Opportunities (AFO). The Flight Opportunities Program, through NASA’s Office of the Chief Technologist (OCT), seeks to provide flight opportunities for “payloads maturing crosscutting technologies that advance multiple future space missions to flight readiness status,” and would be a potential source of funding for the SPORE drop test.

B. Columbia Scientific Balloon Facility

Another potential balloon launch provider is the Columbia Scientific Balloon Facility, contracted through NASA Goddard’s Wallops Flight Facility. The CSBF is based in Palestine, Texas, and has operated for over 40 years and launched more than 2000 stratospheric balloons for universities, agencies, and foreign groups. The facility is capable of launching out of Palestine, Texas in addition to remote locations within the US (including Alaska and Hawaii), Antarctica, Argentina, Australia, Brazil, Canada, India, New Zealand, Sicily, and Sweden.²

The SPORE drop test is considered a conventional CSBF balloon flight, with its short flight duration and use of direct line-of-sight electronics for command and data handling. Most conventional flights are launched from Palestine, Texas; Ft. Sumner, New Mexico; Lynn Lake, Canada; and Kiruna, Sweden, and sometimes Australia and Alaska.² The CSBF provides a relationship between a given conventional high altitude balloon volume, suspended weight, and float altitude (see Figure 1). As will be described in Section V, the capabilities of the 0.11 mcm balloon provided sufficient float altitudes to meet the SPORE drop test requirements. This is ideal, as balloon cost is typically a function of its volume.

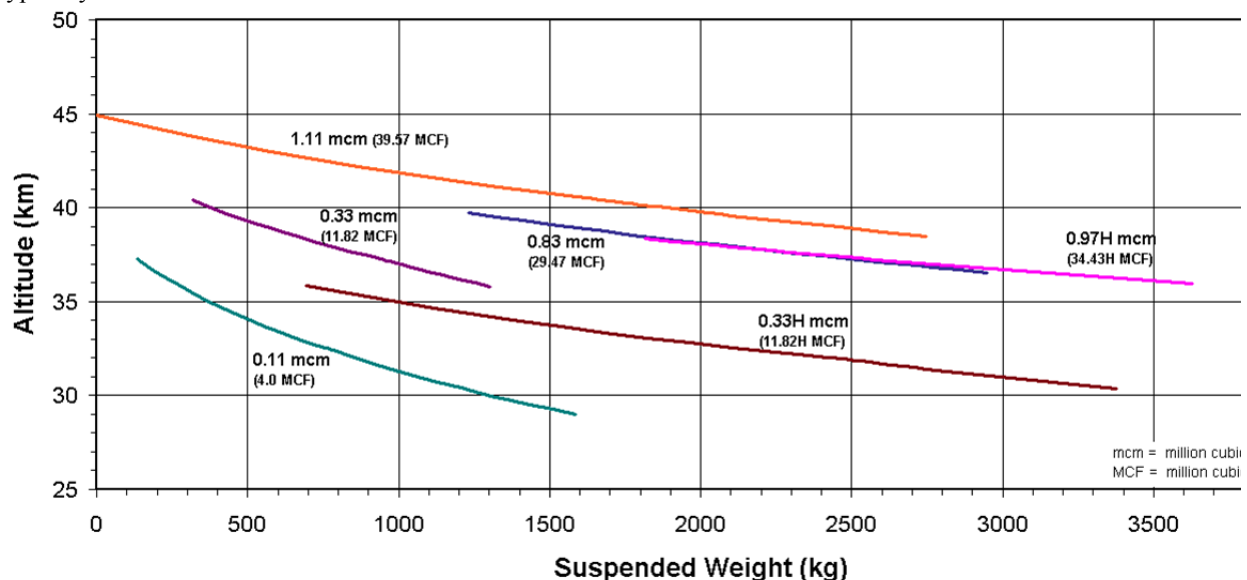


Figure 1: NASA Standards for HAB Float Altitude as a Function of Suspended Weight for Various Balloon Volumes²

The CSBF provides flight support for all launch customers, planning and developing facilities to meet balloon flight support requirements and providing operational services before, during, and after launch. For a typical balloon launch, these operational services include inflating the balloon, launching the balloon and payload, providing telecommand services and data retrieval, and tracking and recovering the payload. In addition to basic flight operations support, the CSBF can also provide engineering support on areas such as balloon systems design, electronics design, gondola design, payload and gondola thermal analysis, power subsystem design, instrumentation design and integration, and recovery system design. For NASA-sponsored customers, the CSBF also provides the balloon, helium, rigging, electronic interfacing, flight and staging facilities, and services directly associated with flight support (most be paid for by non-NASA sponsored users).² A more detailed description of the typical launch and ground operations can be found in Section VIII, and more information regarding CSBF procedures and documentation can be found in their Conventional Balloon Flight Procedures Users Handbook² and their website: www.csbf.nasa.gov.

V. Test Configuration Trade Study

In order to design a high-altitude balloon drop test of the SPORE entry system, a trade study was performed to select the desired test setup and conditions. This analysis was used to determine parameters such as the necessary balloon volume, float altitude, system mass, and parachute deployment timer settings. The tool used for the subsequent trade studies involved a three degree-of-freedom (3-DOF) trajectory simulation, a parachute drag and inflation model, an aeroshell drag model, a standard atmosphere model, and an atmospheric winds model, all of which are described in the following sections.

A. 3-DOF Trajectory Simulation

A 3-DOF simulation of drop test probe and parachute trajectory was written, that includes non-planar and rotation effects. The kinematic and force equations of motions are shown in Equations 1 through 6 below. (Source 17, Vinh) A description of each variable can be found in the Nomenclature Section. Note that normal forces on the vehicle (due to lift) were neglected because the body was assumed to always be at 0° angle of attack.

$$\frac{dr}{dt} = V \sin \gamma \quad (1)$$

$$\frac{d\theta}{dt} = \frac{V \cos \gamma \cos \psi}{r \cos \phi} \quad (2)$$

$$\frac{d\phi}{dt} = \frac{V \cos \gamma \sin \psi}{r} \quad (3)$$

$$\frac{dV}{dt} = -\frac{D}{m} - g \sin \gamma + \omega^2 r \cos \phi (\sin \gamma \cos \phi - \cos \gamma \sin \phi \sin \psi) \quad (4)$$

$$V \frac{d\gamma}{dt} = -g \cos \gamma + \frac{V^2}{r} \cos \gamma + 2\omega V \cos \phi \cos \psi + \omega^2 r \cos \phi (\cos \gamma \cos \phi + \sin \gamma \sin \phi \sin \psi) \quad (5)$$

$$V \frac{d\psi}{dt} = -\frac{V^2}{r} \cos \gamma \cos \psi \tan \phi + 2\omega V (\tan \gamma \cos \phi \sin \psi - \sin \phi) - \frac{\omega^2 r}{\cos \gamma} \sin \phi \cos \phi \cos \psi \quad (6)$$

By numerically integrating these equations using a small time step (0.1 seconds) one can estimate the trajectory of the drop test vehicle with a computation time that is reasonable for Monte Carlo analyses.

B. Parachute Model

The main parachute for the SPORE entry vehicle is a mortar-deployed, cross-type parachute manufactured by Pioneer Aerospace, for use on 16kg flares. It provides enough drag force to decelerate the vehicle to a required 5 m/s

touchdown velocity to avoid damage to the thermal protection system. The chute has a nominal diameter of 4.5 m and a nominal drag coefficient of 0.675. A side view of a typical cross parachute can be seen in Figure 2 below.

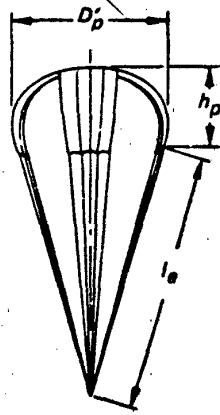


Figure 2: Inflated profile of cross-type parachute.¹

For the test condition trade study and Monte Carlo analyses, several assumptions were made regarding the parachute, because of limited information. The combined length of the bridles, suspension lines, and riser was assumed to be 5 nominal diameters (as is typically with subsonic, cross-type parachutes). In addition, the mortar ejection force was assumed to be 10 N and was assumed to provide a 10 m/s relative ejection velocity.

Because parachute inflation for SPORE takes place in a dense atmosphere with a light vehicle, significant deceleration will occur during inflation, and so it cannot be assumed to be an infinite mass process. A standard model for parachute inflation is the Pflanz inflation model, which was used for the SPORE drop test parachute.¹ Equation 7 below shows the Pflanz relationship between parachute force (F_p) and various parachute characteristics, including the nominal chute drag area ($C_{Do}S_o$), the opening force factor (C_X), the canopy fill constant (n), time of line stretch (t_{LS}) and the time of full chute inflation (t_{FI}).

$$F_p(t) = q(C_{Do}S_o)C_X \left(\frac{t - t_{LS}}{t_{FI} - t_{LS}} \right)^n \quad (7)^1$$

The opening force factor accounts for the overshoot in drag force experienced by most parachute inflation processes, whereas the canopy fill constant gives the correct shape to the inflation profile and is based on empirical relationships. Both are a function of canopy type, and for an infinite mass inflation scenario, both can be assumed to be constant. However, because the drop test inflation would be better approximated as a finite mass inflation, C_X was assumed to vary as a function of the parachute canopy loading factor, or the vehicle weight over the parachute drag area ($m_{vehicle} g / C_{Do}S_o$). For the SPORE drop test article, the canopy loading factor is around 9.6 N/m², and using a relationship from Knacke et al.¹, the opening force factor reduction is nearly 95%! Therefore, a value of 0.1 was used for C_X and 11.7 was used for n (both based on empirical data from Knacke et al.¹ for cross-type parachutes). The values for time of line stretch (t_{LS}) and time of full inflation (t_{FI}) were found using Equations 8 and 9 shown below.

$$t_{LS} = \frac{l_{lines}}{V_{eject}}, \quad t_{FI} = \frac{nD_o}{V_{LS}} \quad (8) \quad (9)^1$$

Here l_{lines} is the combined length of the bridle, riser, and suspension lines, V_{eject} is the relative parachute ejection velocity, D_o is the nominal parachute diameter, and V_{LS} is the vehicle velocity at line stretch.

C. Aeroshell Drag Model

The geometry for the SPORE re-entry probe was taken from the Mars Microprobe geometry, featuring a 45-degree spherecone with a hemispherical afterbody whose radius of curvature is centered at the vehicle's center of gravity (for forward-reorienting stability purposes, see Mitcheltree et. al¹³). The geometric relationships for this aeroshell are shown in Figure 3.

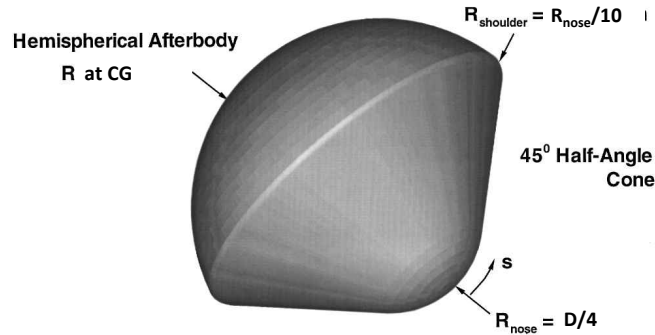


Figure 3: SPORE Re-entry Probe Geometry (Mars Microprobe)¹³

A drag profile for the entry vehicle was constructed using the various wind tunnel and CFD data used in similar analyses for the Mars Microprobes.¹³ The drag models included in the POST program for a forty-five degree spherecone were also used to construct the SPORE drag model. Figure 4 shows a plot of the SPORE drag model, along with wind tunnel data, CFD LAURA data, and the Newtonian flow solution for hypersonic velocities.

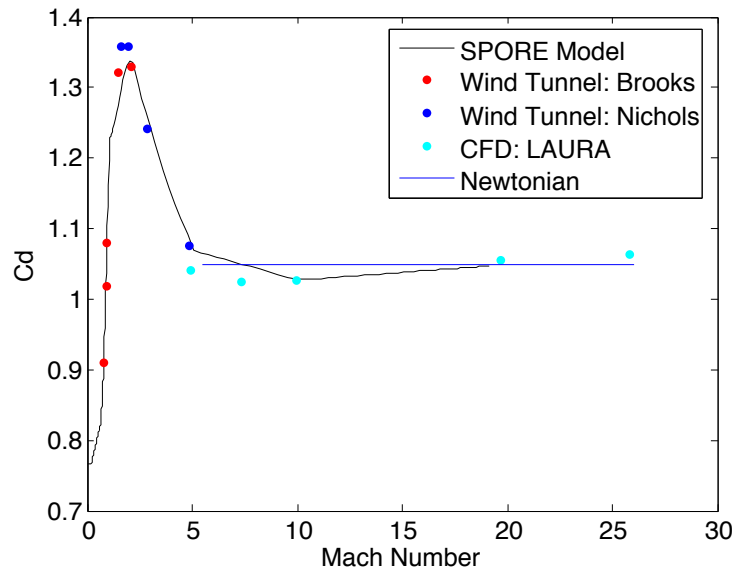


Figure 4: Drag Profile for 45° Spherecone.¹³

For Mach numbers above 20, the drag coefficient was assumed to be constant at 1.048. This drag model was then used for both the test condition trade study and Monte Carlo analyses of the drop test.

D. Atmospheric Winds Model

In both the trade studies and Monte Carlo analyses, atmospheric winds were included in the vehicle's Earth-relative velocity. A winds model was taken from Hedlin et al.⁶ for mesospheric and stratospheric winds at 30 to 60°N latitudes (assuming a launch out of New Mexico or Texas). The wind speed as a function of altitude can be seen in Figure 5. As will be explained in the Monte Carlo Uncertainty Characterization section, an uncertainty (and therefore 6-sigma offset) of 10 m/s was assumed for the winds profile, because all of the drop test conditions occur in the stratosphere.

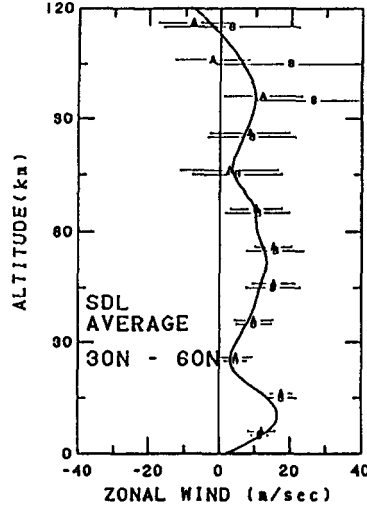


Figure 5: Empirical Atmospheric Winds Profile for 30 to 60°N.⁶

To include the effects of wind speed on the vehicle’s relative velocity, the wind speed component for a given altitude was simply included in the horizontal vehicle velocity. The winds, zonal and meridional, were assumed to be strictly horizontal to simplify the simulations. Equation 10 shows the Earth-relative vehicle velocity, updated to include winds, where V is the vehicle velocity before winds and V_{winds} is the estimated wind speed.

$$V_{total} = \sqrt{(V_{winds} + V \cos \gamma)^2 + (V \sin \gamma)^2} \quad (10)$$

E. Defining the SPORE Parachute Deployment Conditions

The drop test was designed to provide flight-like dynamic pressures and Mach numbers at parachute deploy in order to verify parachute and parachute system functionality. The nominal LEO return trajectory for a SPORE TPS testbed mission has the entry state characteristics shown in Table I below, with the values for initial velocity, altitude, flight path angle, latitude, longitude, heading angle, and mass all listed respectively.

Table I: SPORE LEO, TPS Testbed Nominal Entry State

Parameter	Value	Units
V_o	7780	m/s
h_o	125	km
γ_o	-5.0	°
ϕ_o	137.65	°E
θ_o	-16.65	°N
ψ_o	267.10	°
m_o	10.51	kg

For this trajectory, the main parachute is deployed subsonically at a desired deployment Mach number of 0.8, which will be targeted using a timer and a G-switch. At this deployment condition, the approximate dynamic pressure is 1.0088 kPa. An altitude versus velocity plot of this nominal LEO trajectory is shown in Figure 6 below, with a callout for parachute deploy.

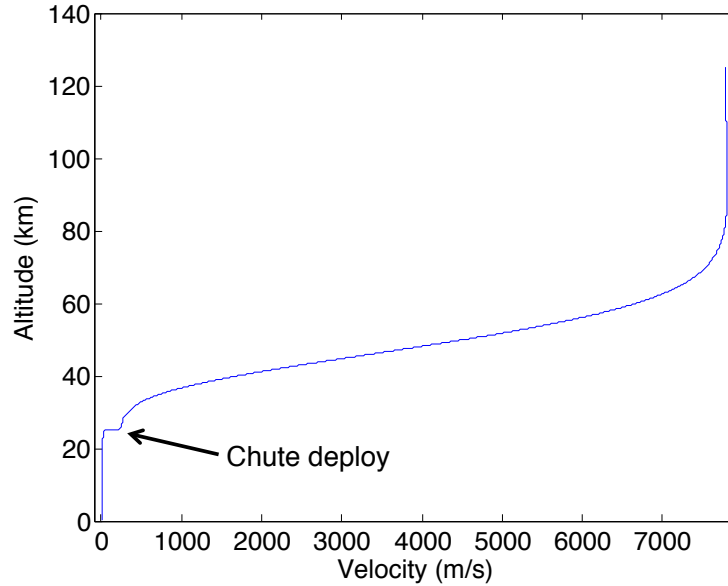


Figure 6: SPORE Nominal LEO TPS Testbed Trajectory.

F. Defining the Drop Test Conditions

A trade study was performed on drop test initial conditions in order to achieve flight-similar dynamic pressures and Mach numbers at parachute deployment. By varying balloon float altitude (which is a function of suspended mass), the potential energy of the drop test system can be varied to achieve different test conditions. The standard NASA relationship between float altitude and suspended weight was taken from the data in Figure 1 for a 0.11 mcm balloon. The 0.11 mcm balloon turned out to provide sufficient altitude to meet test conditions and was also ideal because drop test cost is typically a function of balloon volume.

To find the best drop test conditions, balloon float altitude was varied from 37.5 km to 29 km, for both a scenario with winds and without winds, to compare the differences. For the no-winds scenario, the optimal suspended mass was 577 kg, which can achieve a float altitude of 33.62 km with a 0.11 mcm balloon. This initial condition reaches a dynamic pressure of 1.0101 kPa at a Mach number of 0.8115 at 45.3 seconds after separation from the gondola. A plot of the dynamic pressure and Mach number for varying float altitudes is shown in Figure 7, with the best-fit trajectory highlighted in cyan and the parachute deployment condition shown with a red marker.

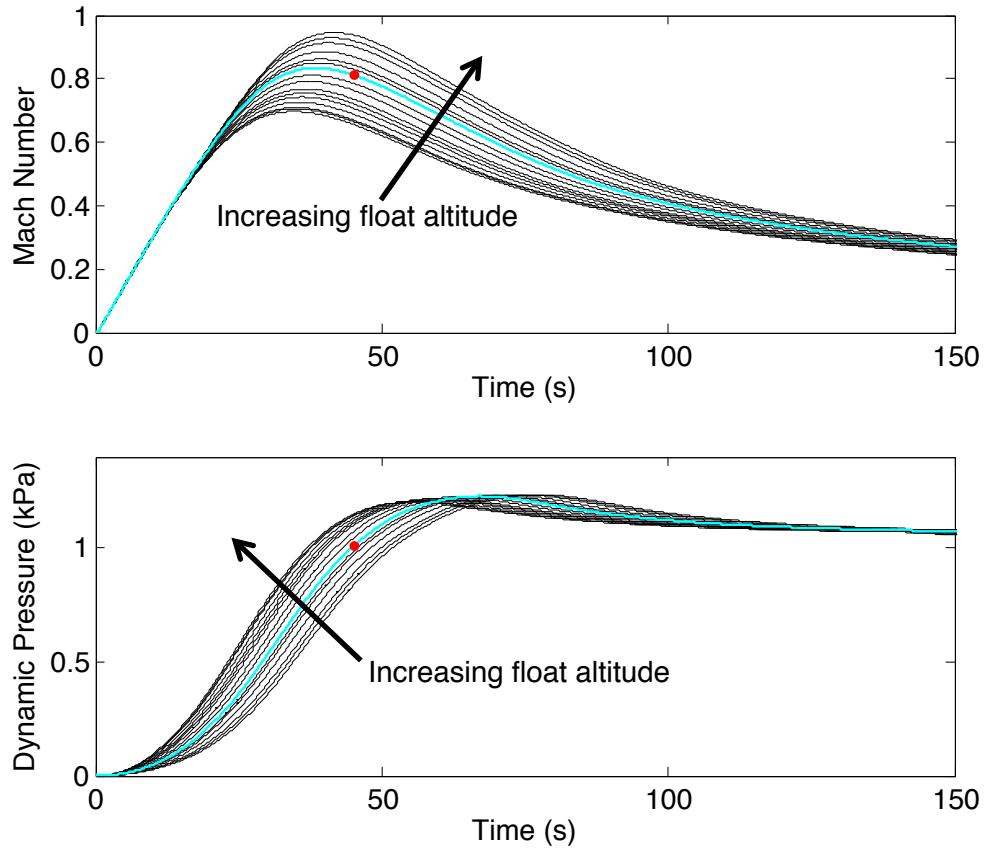


Figure 7: Sweep of float altitude for 0.11 mcm balloon. Desired chute deployment condition highlighted in red on cyan trajectory.

However, with winds included in the trade study, the best-fit test condition is slightly different. The best balloon float altitude is at 32.821 km, requiring a suspended mass of 726.09 kg. With this initial altitude, the vehicle reaches a parachute deployment condition 43 seconds after gondola separation, with a dynamic pressure of 1.0045 kPa and a Mach number of 0.7979, as shown in Figure 8. With the addition of the winds into the trajectory simulation, the dynamic pressures experienced by the vehicle are higher during the lower-altitude portions of the trajectory, rather than at the higher velocity segments at higher altitudes.

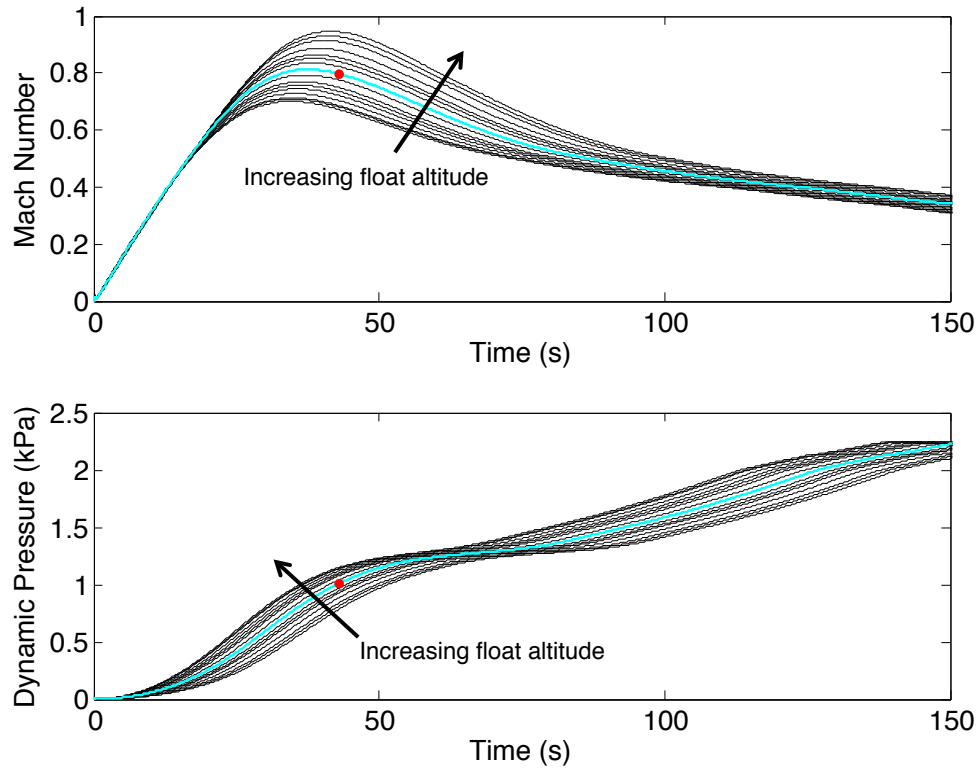


Figure 8: Sweep of float altitude for 0.11 mcm balloon (with winds). Desired chute deployment condition highlighted in red on cyan trajectory.

Because including winds in the model was found to cause significant differences in the initial test conditions, the second test condition (at 32.8 km float altitude) was assumed for the actual drop test.

VI. Monte Carlo Analysis

In order to investigate the effects of various test conditions on parameters such as parachute deployment conditions and landing footprint, a Monte Carlo analysis was performed for the SPORE drop test. Large amounts of output and input data were needed, and so 500 cases were selected to save on memory but also capture the final distributions of the various outputs.

A. Uncertainty Characterization

To account for the uncertainties associated with many of the test parameters, distributions of values were assumed for the Monte Carlo analysis. Table II details the distributions assumed for each parameter, along with their mean value and standard deviation (for normal distributions) or upper and lower bounds (for uniform distributions).

Table II: Varying Parameters and Their Distributions Used in Monte Carlo Analysis.

Parameter	Description	Units	Distribution Type	Mean Value	Standard Deviation	Upper Bound	Lower Bound
h_o	Float altitude	km	Normal	32.82	0.033	N.A.	N.A.
ϕ_o	Drop latitude	deg N	Normal	31.76	0.15	N.A.	N.A.
θ_o	Drop longitude	deg E	Normal	-95.63	0.15	N.A.	N.A.
ψ_o	Initial heading	deg	Uniform	N.A.	N.A.	0	360
D_o	Nominal chute diam.	m	Normal	4.5	0.0167	N.A.	N.A.
C_{D_o}	Chute drag coefficient	--	Normal	0.675	0.0083	N.A.	N.A.
t_d	Time to chute deploy	s	Normal	40.9	0.1667	N.A.	N.A.
F_S	Snatch force	N	Normal	3000	100	N.A.	N.A.
F_{eject}	Mortar ejection force	N	Normal	10	1.667	N.A.	N.A.
V_{eject}	Mortar ejection velocity	m/s	Normal	10	0.833	N.A.	N.A.
m_o	Vehicle initial mass	kg	Normal	10.51	0.35	N.A.	N.A.
V_{winds}	Wind velocity	m/s	Normal	0	5	N.A.	N.A.

For several of the parameters, the standard deviations were selected such that the 6-sigma values were within the estimated upper and lower bounds. For h_o an uncertainty in the float altitude of +/- 100 m was assumed, whereas for the nominal parachute diameter (D_o) an uncertainty of +/- 5 cm was assumed. The parachute drag coefficient was given as a range from 0.65 to 0.70, and so a mean value of 0.675 with a 6-sigma offset of 0.025 was assumed. The time of parachute deploy was assumed to potentially occur 1/2 a second before or after the desired time, to account for inaccuracies in the timer. Because the parachute snatch force varies with deployment dynamic pressure, it was assumed to have a 10%, or 300 N variation about the mean. The mortar ejection force was assumed to vary by 50% and the ejection velocity, by 25%, because of a lack of information regarding the mortar capabilities. Because the probe mass has not been fully characterized, a mean value of 10.51 kg was used to match the actual SPORE vehicle mass, with a 10% variation.

The initial heading angle, ψ_o , was assumed to have a uniform distribution from 0° to 360° , because the drop test initiates in a nearly-vertical configuration, and so depending on the zonal and meridional winds, the probe could potentially have a heading angle in any direction. This initial heading angle, however, doesn't have much of an effect on the test outcomes, because the initial flight path angle is 90° to within $\frac{1}{2}$ a degree.

As mentioned in the Test Configuration Trade Study section, an atmospheric winds model was taken from Hedlin et al. for zonal and meridional winds at 30 to 60°N latitudes. Hedlin characterized the overall root mean square differences between all of the data used to create his model as being on the order to 15 m/s in the mesosphere (85 km to 50 km altitudes) and 10 m/s in the stratosphere (50 km or less).⁶ Because all drops investigated occurred at less than 50 km , the stratospheric RMS value of 10 m/s was used as the 6-sigma value for the wind speed distribution.

The driving factor for variations in initial latitude and longitude is balloon drift, which can be quite significant for high altitude balloon tests. In order to characterize the bounds on balloon drift, values of observed drift were taken from similar historical tests. For example, for the Huygens HASI Balloon Drop Test, the balloon drifted within a radius of 50 km during the whole of ascent, float, and descent. Figure 9 shows the drift profile measured during the HASI drop test. This test had a float altitude of approximately 32 km (close to the SPORE target float altitude) and took place over a period of 3.6 hours.³ Similarly, the Viking PEPP parachute drop tests observed a maximum balloon drift of 39.3 km (See Figure 10) for tests performed at White Sands, New Mexico with a 39 km target float altitude.¹⁵ Based on these two historical observations, a max drift radius of 50 km was assumed (as a worst-case scenario), which is equivalent to a 0.45 degree change in latitude and longitude. This 0.45 degrees was used as the 6-sigma offset for the Monte Carlo initial latitude and longitude values. The mean values were assumed to be the location of the CSBF facility in Palestine, Texas.

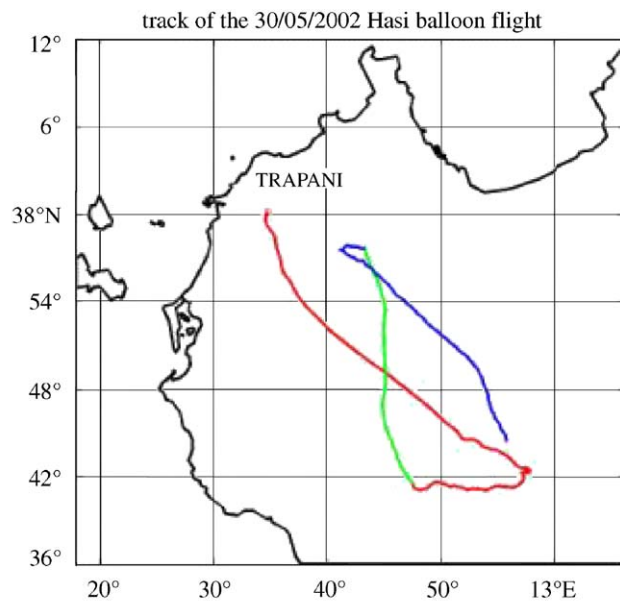


Figure 9: Balloon drift profile for Huygens HASI drop test.

(red = ascending, green = float, blue = descending)³

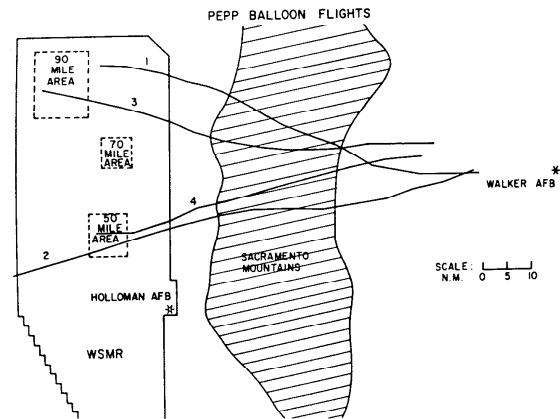


Figure 10: Viking PEPP balloon drift profiles.¹⁵

B. Results

Using the distributions listed in Table II, a 500-case Monte Carlo analysis was performed. As expected, the variability in the initial conditions resulted in variability of the vehicle trajectory and parachute deployment conditions. In Figure 11, the vehicle altitude versus velocity is plotted for all 500 cases. One can see that the horizontal “band” at which the vehicle decelerates from parachute inflation covers approximately 2.5 km , so there is significant variety in parachute deployment altitude.

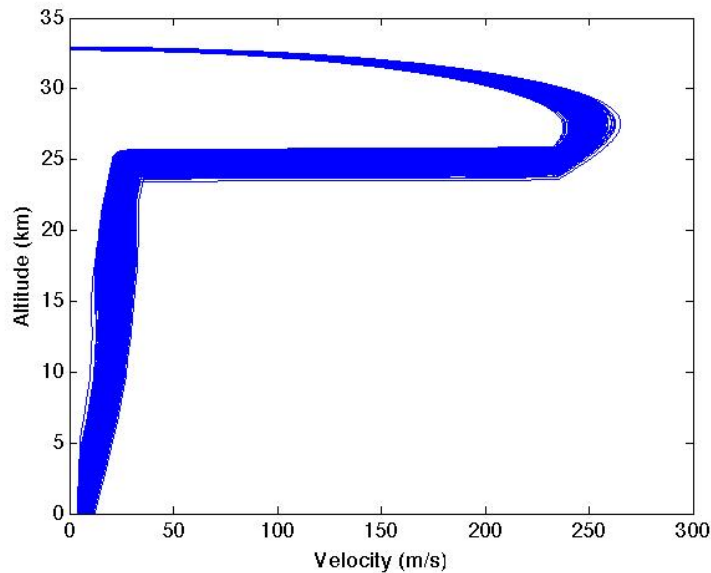


Figure 11: Altitude vs. Velocity for Full Swath of Monte Carlo Trajectories.

To capture the variability in parachute deployment conditions, histograms of the dynamic pressure, altitude, and Mach number at mortar fire were generated, as can be seen in Figure 12. The dynamic pressure distribution captured the desired condition (1008 Pa), and ranged from values of 894 Pa to 1323 Pa and was skewed to the lower values. The altitude of mortar fire ranged from 24.2 km to 26.4 km and was skewed to the high altitudes. Finally, the Mach number at mortar fire ranged from 0.7737 to 0.8307, and is centered around the target value of 0.8.

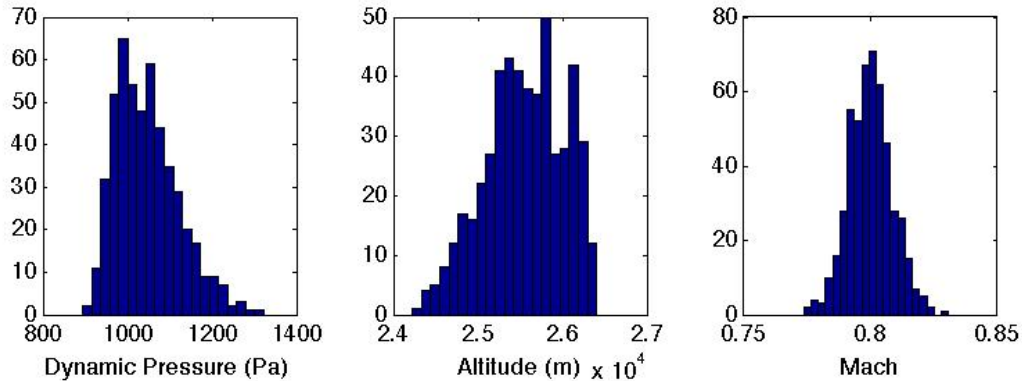


Figure 12: Parachute Deployment Conditions (Distributions).

Figure 13 shows the correlation between the Mach number and dynamic pressure at mortar fire for each of the 500 cases. The desired condition is highlighted in red. As one can see, the scatter is relatively centered about the target value, with minimal spread on the deployment Mach number (approximately $\pm 3\%$). There is larger variability associated with the deployment dynamic pressure, ranging up to 31% higher than the target value. This is something that could be adjusted with a more accurate mortar timer or better control over float altitude. However, because most of the off-nominal cases are at larger dynamic pressures (i.e. more stressful conditions for the canopy), one would be more certain of parachute functionality for the actual SPORE deployment conditions.

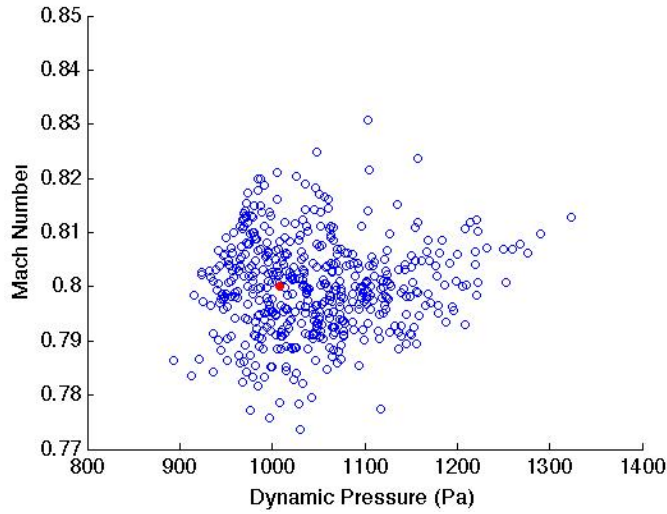


Figure 13: Scatter of Mach Number and Dynamic Pressure at Chute Deployment. Target Value Highlighted in Red.

The final goal of the Monte Carlo analysis was to characterize the drop test vehicle landing ellipse. Because the vehicle is Earth-facing at gondola release (-90° flight path angle), the largest driving factor of landing ellipse size is the initial latitude and longitude distribution because of balloon drift. A scatter of the latitude and longitude of the vehicle at touchdown is shown in Figure 14, with the mean value highlighted in red. Taking the extremes of both latitude and longitude yields a landing ellipse of 108.26 km North-South and 111.79 km East-West. This ellipse would be acceptable for a CSBF launch out of Palestine, Texas and would fall within their 200-mile payload drop-radius requirement.²

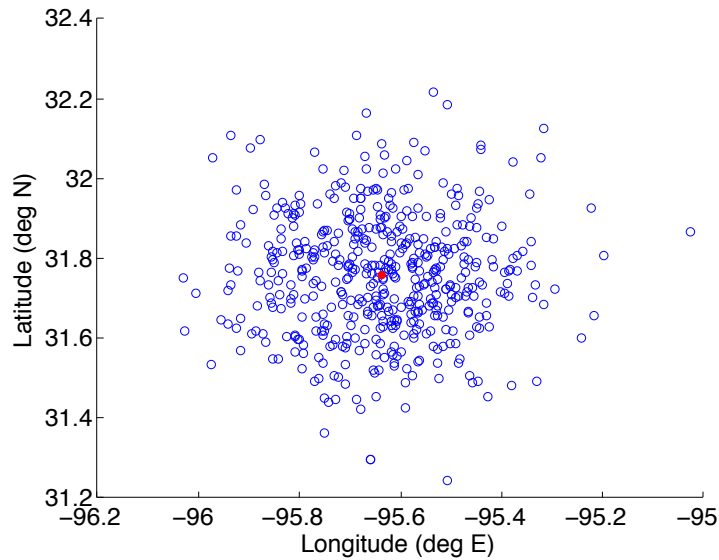


Figure 14: EDL Landing Ellipse, Center Highlighted in Red.

VII. Test Vehicle Design

A. Entry Capsule Design

The entry probe for the SPORE drop test would be very similar to the actual 1-U SPORE vehicle in terms of mass, geometry, and hardware. The SPORE 1-U entry vehicle has a max diameter of 16 inches (to provide 1:1 geometric similitude with TPS arcjet testing models), and has a current best estimated mass of 10.51 kg. Using hardware that is as similar to flight hardware as possible would be desired in order to demonstrate the system functionality. Of course, additional instrumentation would be needed, that would provide test-specific data. The original 1-U SPORE packaging model features the 45-degree spherecone base structure covered in the forebody and aftbody TPS. Internal to the structure is a circular shelf onto which all electronics and hardware are mounted. The parachute, packaged in the mortar takes up the largest internal volume and would extend through a central cut-out in the shelf. At the nose of the vehicle is an aluminum ballast that also serves as a heat sink to protect the electronics. Attached to the top of the shelf would be all of the internal electronics: the batteries, PDU, comms antenna and receiver, and data processing and storage devices. These are all of the hardware currently included in the SPORE 1-U packaging model.

In addition to the standard hardware, the drop test probe would feature an up-looking camera, mounted to the aftbody structure and protruding slightly through the aftbody TPS. This would be offset from the vehicle centerline to avoid the parachute mortar cap during parachute deployment. The camera would provide video footage of the parachute deployment, inflation, and dynamical behavior throughout the process. For the mass budget, the Allied Pike F-100 CCD camera was used as a placeholder (this camera could be a viable option, as it provides outstanding image quality and high frame rates). In order to back out the probe's dynamical behavior during the drop test, a 3-axis accelerometer and 3-axis rate gyro would also be used. As a placeholder, the Arduino 3-axis accelerometer (ADXL-345) and their triple-axis digital output gyro (ITG-3200 Breakout) were used in the mass budget. These two chips are extremely lightweight (<2mg) and would provide digital output to be interfaced with the processor. To monitor hardware temperatures, several thermocouples would also be integrated into the drop test probe, and to determine the freestream stagnation, static, and dynamic pressures, a differential pressure transducer would be mounted to the vehicle nose, protruding through the forebody TPS. For the mass budget, the Omega PXM409-350HGV differential pressure transducer was used as a placeholder. Finally, as an option for vehicle altitude, latitude, and longitude knowledge, a GPS receiver and antenna could also be included in the drop test probe. The Surrey Satellite Technology SGR05 GPS receiver and antenna were used in the mass budget. A preliminary cross-sectional view of the drop test probe packaging can be seen in Figure 15, with callouts to major hardware. In addition, a preliminary mass budget of the drop test probe was developed and is shown in

Table III. As one can see, the total system mass is very similar to the actual entry vehicle mass of 10.51kg.

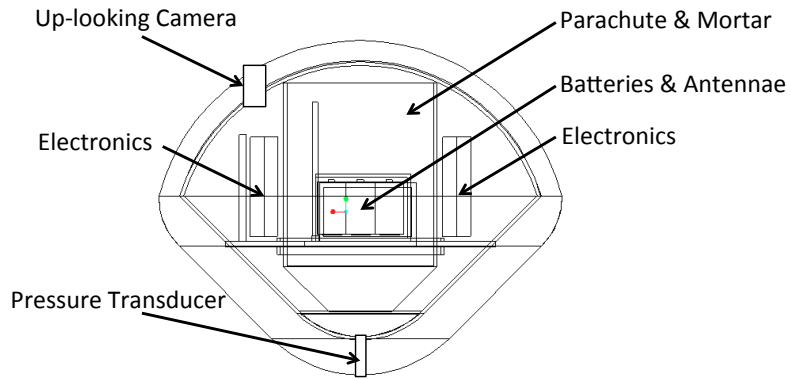


Figure 15: Preliminary Drop Test Probe Packaging Model.

Table III: Approximate Mass Budget for Drop Test Entry Probe.

Component	CBE (kg)
Forebody Structure	0.960
Aftbody Structure	1.080
Forebody TPS	1.200
Aftbody TPS	0.400
Component Shelf	0.540
Primary Batteries (3)	0.260
Power Control Board/Battery Mounting	0.450
Camera	0.250
3-Axis Accelerometer & Casing	0.015
Differential Pressure Transducer	0.200
Temperature Sensors	0.020
Triple Axis Rate Gyro & Casing	0.018
Processor (with Flash Memory)	0.650
Antennae	0.220
Comms Transmitter	0.310
GPS	0.020
Parachute & Canister	1.440
Mortar	1.470
Heatsink/Ballast	1.010
Total Mass	10.513

B. Gondola Design

The purpose of the drop test gondola is to provide a mechanical and electrical interface between the probe and the rest of the ascent train. The gondola also carries all additional instrumentation and hardware not internal to the probe, and can provide an additional communications link between both the ground and the probe. For the SPORE drop test, a relatively simple gondola design would be required. A drawing of a gondola concept for the SPORE drop test can be seen in Figure 16. The gondola structure could be a simple truss structure with a hexagonal shelf for mounting all hardware. At the gondola base, a series of support bars would mechanically attach to the outer diameter of the drop test probe. Upon ground command, a series of pyrotechnic bolts would fire, detaching the probe from the gondola. At the top of the gondola structure there would be a mechanical attachment to the suspension cables that are then connected to the rest of the ascent train.

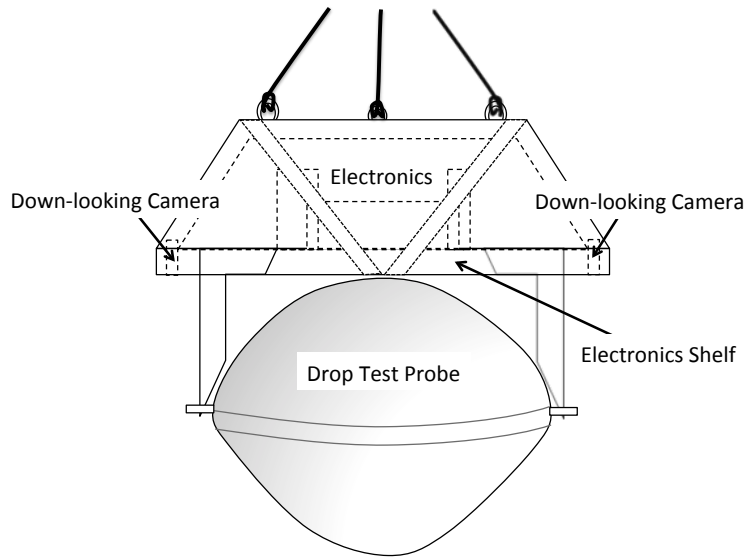


Figure 16: Preliminary SPORE Drop Test Gondola Design.

In terms of hardware, the gondola could have a single or multiple down-looking cameras to provide footage of probe separation. The gondola could also carry a GPS receiver and antenna, to provide differential GPS capability with the probe during its descent. Data storage and handling devices could also be mounted to the gondola shelf, along with the launch provider CIP, an electronics interface which provides a ground-to-balloon telemetry link for transmitting command, tracking, and telemetry signals to and from the payload.

VIII. Ground and Launch Operations

An overview of basic pre-flight, launch, ascent, descent, recovery, and post-flight operations are described in the proceeding sections. This information largely comes from the CSBF *Conventional Balloon Flight Support: Balloon Flight Application Procedures User Handbook*², but is relatively standard for all high altitude balloon launch providers.

A. Pre-Flight Activities

Before a high altitude balloon test is considered flight-ready, the test program must undergo a variety of inspections, certifications, and meetings. In the early stages of test program development, the science group (or customer) holds a Flight Requirements Meeting with the launch provider staff to review the mission's minimum success criteria, in order to set forth the facilities requirements and maintain that minimum success is realistic. Under the CSBF process, the customer is then provided a CIP (electronics interface), which provides a ground-to-balloon telemetry link for transmitting command, tracking, and telemetry signals to and from the payload. Next, the customer undergoes a Gondola Design Certification, ensuring that the gondola adheres to all FAA and NASA Safety standards, as well as launch provider gondola structural, thermal, fastener, and pressure vessel requirements. If radioactive materials are present in the payload, a Radioactive Material Inspection is held to monitor radioactive sources and acquire a Nuclear Launch Safety Approval from the NASA Balloon Program Office.²

After the payload is integrated with the CIP, the launch provider electronics personnel perform an Interface Compatibility Check of the electronics interfaces. The Flight Operations personnel also conduct a Rigging Equipment Check, in which all ascent train equipment are selected, pull-tested, and certified as flight-ready. Meteorological activity is monitored daily in order to identify balloon launch opportunities, and after flight-readiness, daily Flight Status Meetings are held to review launch priority, flight opportunities, and weather forecasts. Once the flight system is considered flight-ready and a launch date is set, the gondola final weight is taken with the PI's sign-off. No more than 72 hours prior to launch, a Flight Readiness Review is held, in which the entire flight train's mechanical and electrical compatibility is certified and flight profile is confirmed. The launch window is defined, as well as the gondola and payload recovery operations.²

B. Launch and Flight Activities

On the day of launch, the Campaign Meteorologists use current and predicted weather conditions to estimate the launch window. The launch support personnel then pick up the balloon payload using a mobile launch vehicle, shown in Figure 17, and the customer and launch personnel perform a check of all electronic interfaces in the staging area. After checkout, the mobile launch vehicle carries the payload to the launch pad, and all remaining flight line checkouts and payload preparations are performed.²

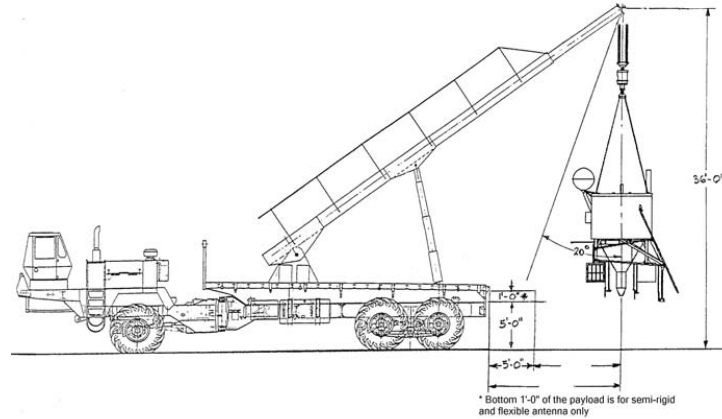


Figure 17: Mobile Launch Vehicle.²

If weather conditions hold, the flight train is assembled and checked out on a protective ground cloth. The flight train equipment and parachute are laid out, and the parachute stream is checked for any damage. The balloon is laid out next and attached to the parachute and the spool vehicle (See Figure 18). After the ascent train is fully checked out, balloon inflation begins. A pre-calculated amount of helium is pumped into the balloon through helium valves (not fully inflating, to allow room for expansion during atmospheric rise). After inflation, the balloon is released from the spool vehicle and the payload is maneuvered perpendicularly below it. After the balloon is directly above the payload and Mobile Launch Vehicle, the payload is released and begins its ascent to the desired float altitude, thus concluding the balloon launch. A concept for the SPORE ascent train can be seen in Figure 19.

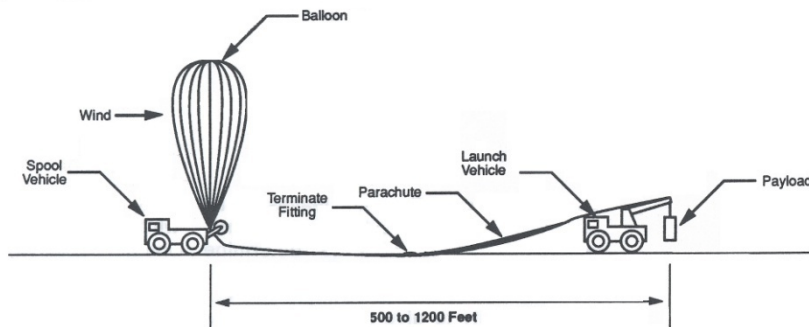


Figure 18: Flight Train and Balloon Layout.²

Data collection and command control is maintained from pre-launch until payload recovery. After the float altitude is reached, the probe is separated from the support gondola via ground control. After the probe has been safely separated, the parachute recovery system deploys upon ground command, deflating the balloon and carrying the gondola to the ground for recovery. The gondola, balloon carcass, and probe are all recovered by the ground crew, returning the probe to the customer. After completion of the balloon flight, the PI fills out a post-flight assessment form before leaving the launch site, and the customer receives all downlinked and stored data relevant to their science mission.



Figure 19: Concept for SPORE Drop Test Ascent Train (Not to Scale).

IX. Conclusions

In conclusion, a high altitude balloon drop test of the SPORE Earth entry vehicle was presented as a means of testing parachute functionality at flight-like conditions, re-entry dynamics and stability, as well as entry system functionality. The final drop test probe mass was estimated to be 10.51 kg, and would require a drop from 32.8 km altitude from a 0.11 mcm balloon in order to achieve flight-like dynamic pressure and Mach number at parachute deploy, based on a trade study of varying float altitudes and balloon volumes. The landing ellipse size and variability of parachute deployment conditions were characterized using a Monte Carlo analysis on the drop test trajectory. In addition, a preliminary gondola and probe design were described, as well as a description of standard pre-flight and flight procedures for high altitude balloons. As a helpful reference, data was also gathered from similar historical drop test programs and is included, as it greatly influenced the SPORE drop test design.

Appendix A: Historical Balloon Drop Tests

Program Name	Mars Subsonic Parachute Tests	Galileo Probe Drop Test	Galileo Probe Drop Test	Huygens Probe Drop Test	Huygens HASI 2002 Balloon Campaign	Stardust Systems Drop Test	Hayabusa (MUSES-C) Drop Tests	Hayabusa (MUSES-C) Drop Tests
Planet	Mars	Jupiter	Jupiter	Titan	Titan	Earth-return	Earth-return	Earth-return
Year	2004	1982	1983	1995	2002	1998	1996	1998
Facility Name	National Scientific Balloon Facility	White Sands Missile Range	White Sands Missile Range	French Space Agency; landed in Esrance, Sweden	Italian Space Agency Base "Luigi Broglio"	Utah Test and Training Range	Sanriku Balloon Center	Sanriku Balloon Center
Location (City, State, Country)	Ft. Sumner, NM, USA	White Sands, NM, USA	White Sands, NM, USA	Esrance, Kiruna, Sweden	Sicily, Italy	Utah, USA	Iwate, Japan	Iwate, Japan
Number of Drops	4	2	2	1	3	1	2	2
Drop #	4	1	2	1	2	1	1	2
Purpose of Test	Develop new chute system for Mars exploration	Confirm proper parachute operation	Confirm proper parachute operation	Demonstrate parachute deployment sequence; characterize probe stability and spin design features	Test spare sensors of HASI experiment in dynamic conditions, use trajectory reconstruction algorithm, test probe-parachute system motion	Verification/observation of main chute deployment, spacecraft computer and sensor performance, test facility demo	Verify proper function of parachute deployment system; examine transonic aerodynamics	Verify proper function of parachute deployment system; examine transonic aerodynamics
Balloon Volume (m ³)	340000	141584	141584	Unk	98862	Unk	30000	Unk
Target Float Altitude	36	Unk	Unk	Unk	Unk	Unk	Unk	Unk
Actual Float Altitude	36.6	29.56	29	37.4	32.5	3.96	36	Unk
Ascent Time (hr)	2.5	4	Unk	3	1.83	Unk	Unk	Unk
Ascent Train	Gondola, gondola release mechanism, extended safety chute, terminate release mechanism, balloon	Unk	Unk	Type 402 Z main balloon, auxiliary balloon	Probe (includes gondola) with all instruments, telemetry box about 2.6 m above probe, parachute linked to TM by heavy bifilar line supporting all devices to perform probe release, RAVEN-supplied balloon	Involved flight-similar Parachute Recovery System (PRS) and Sample Return Capsule (SRC), drogue (deployed statically without mortar), main chute, "hot air balloon"	Unk	Unk
Total System Mass (kg)	1134	Unk	Unk	<1000	448	Unk	Unk	Unk
Gondola Design	Truss structure, aerodyn fairing, structural base with instruments, crushable honeycomb, parachute system	Unk	Unk	Bracket interfaces probe and gondola for pyro separation; umbilical separation by lanyard; spin vanes	Spin vanes on gondola to simulate actual spin; lead bricks on top	Unk	Transponder installed	Unk
Gondola System Mass	980	Unk	Unk	Unk	51	Unk	Unk	Unk
Probe Design	N/A	376 kg ballast added to nose	376 kg ballast added to nose	Full-scale probe model with flight-like hardware (SM2)	1:1 scaled mock-up of Huygens probe; ring supporting a double-plate platform, bottom front cone, upper cover	Sample Return Capsule (SRC)	45 degree spherecone	45 degree spherecone. Structural components were upgraded to simulate actual entry vehicle
Probe Diameter (m)	N/A	1.22	1.22	1.5	1.5	0.81	0.4	0.4
Probe Mass (kg)	N/A	210	210	Unk	117	45.36	26	20
Parachute Design	Chute Config.	Two-stage system (Drogue and Main)	Two-stage (Drogue and Main)	Three-Stage (Pilot, Main, and Stabilizer)	Single parachute	Two-stage (Drogue and Main)	Single Parachute, 60% Reefed	Single Parachute
	Drogue Chute Diam (m)	16.1	1.14	1.14	Unk	N/A	0.83	N/A
	Drogue Chute Type	Viking	Conical Ribbon	Conical Ribbon	Unk	N/A	DGB	N/A
	Drogue Chute Geom Porosity (%)	Viking	16.5	16.5	Unk	N/A	Unk	N/A
	Drogue Chute Material	Viking	Heat-set dacron	Heat-set dacron	Unk	N/A	1.1 oz nylon	N/A

	Main Chute Diam (m)	33.5	3.8	3.8	Unk	24	7.3	2.88	2.88
	Main Chute Type	Ringsail	Conical Ribbon	Conical Ribbon	Unk	Hemispherical (Irvin-supplied)	Triconical	Cross Type	Cross Type
	Main Chute Geom Porosity (%)	Unk	22	22	Unk	Unk	Unk	34	34
	Main Chute Material	Unk	Heat-set dacron	Heat-set dacron	Unk	Unk	1.1 oz nylon	Nylon	Polyester; overlap radar reflective cloth
	Deployment Sequence	Static-line deployed drogue after gondola release, timer-triggered main chute w/ pyro cutters	Pilot chute deploy, aft heatshield removal, main chute deploy, descent module sep from decel module	Pilot chute deploy, aft heatshield removal, main chute deploy, descent module sep from decel module	Pilot chute deploy at Mach 1.5, Back cover of aeroshell separated, pulls out main chute; front of aeroshell separated; main chute jettison and smaller stabilizer chute deployed. Separation based on majority voting	Balloon carries ascent train to desired altitude, balloon and chute linked via connector pyro cable fired via ground command; parachute static-line deploys; TM ballast jettisoned via ground command	Static deployment of drogue, computer initiated deployment of main	Gondola release commanded by ground. Parachute cover jettison w/ pyro pushers, deploys cross parachute from toroidal chute container; no HS jettison	Parachute cover jettison w/ pyro pushers, deploys cross parachute from toroidal chute container; HS jettison
	Pyro Specs	Pyro cutters for 3 drogue risers	3 explosive nuts 1.25 s after pilot chute deploy; also sep descent and decel modules		Custom made Pyro Timing and Firing Unit (PTFU) (time-tagged commands); hot redundant Pyro	Pyro cable between balloon and chute	Unk	Pyro Pushers (Double Action) for chute deploy	Pyro Pushers (Double Action) for chute deploy
	Battery Specs	Lithium-ion, sized for 10 hour duration	Has batteries	Has batteries	NiCd rechargeable batteries (for SM2); PDU and Camera Power Supply	Lithium (3V) and Ni-MH (9.6 V) (sustain experiment for 8 h)	Unk	NiCd/NiMH	NiCd
	Telecoms Specs	NSBF Telecom System	Comms with ground	Comms with ground	Ground to gondola (L-band uplink and downlink, radio relay, 400 bps); S-band uplink transmitter (2W) between probe and gondola (15 GHz, link range of 18km); S-band downlink from probe to ground (backup)	Telemetry box located 2.6 m above probe; radar responder, telecoms antenna	Unk	Telemetry	Telemetry
	Camera Specs	2 up-looking (mini-Digital-Video camcorders, 1 hr of video stored on-board), 1 up-looking (connected to telecom for ground storage), downlook (additional), chase plane camera; ground telescope camera	Has cameras to monitor deployment events	Has cameras to monitor deployment events	Film cameras (upward and downward looking)	Unk	Unk	Parachute deployment image (CCD Camera)	Parachute deployment image (CCD Camera)
	GPS Specs	Receiver and antenna included	N/A	N/A	GPS receiver (uses differential GPS (with gondola?))	Has in TM box	Unk	None, location estimated	Unk
	Accelerometer Specs	Northrup Grumman LN-200 IMU (3-axis accelerometers)	Measured chute opening forces	Measured chute opening forces	Has accelerometers	HASI (1 axial Xservo, & 3-axis piezo)	Unk	3-Axis	1-Axis
	Pressure Transducer Specs	5 (3 static behind fairing, 2 were differential (1 at nose))	Unk	Unk	Unk	HASI (4 NOVA pressure sensors, 0-30 kPa internal, 0-7 kPa external)	Unk	Pressures (stagnation and inside)	Inside pressure

Additional Sensors	Record deployment and inflation; load cells on risers; temp sensors on load cells, transducers, and electronics	Instrumentation to monitor deployment, programmer to initiate deployment events, strain gauge	Instrumentation to monitor deployment, programmer to initiate deployment events, strain gauge	Heater mats, thermostats, temp sensors	HASI (two redundant temp sensor units); spare tilt sensor of Huygens Surface Science Package, 3-axis magnetometer, 2 sun sensors; VAISALA meteorological package in TM; 100 kg lead ballast in TM	Unk	"Measurement Electronics"; sequence timer; sequence timing monitor; internal temps	"Measurement Electronics"; sequence timer; sequence timing monitor; internal temps
Rate Gyro Specs	Northrup Grumman LN-200 IMU (3-axis rate gyros)	Has rate gyros	Has rate gyros	Angular rate sensors	Unk	Unk	2-Axis attitude rate sensor and video monitor	2-Axis attitude rate sensor
Data Acquisition and Storage Device Specs	Virtex TM, Field Programmable Gate Array; on-board low power CPU w/ flash storage at 100 Hz	N/A?	N/A?	16 M-byte solid state recorder; PM encoder	integrated data acquisition and instrument control system developed based on PC architecture and soft-real-time application (ins sampled at 1kHz)	Unk	N/A?	Unk
Altitude of Chute Deploy	Unk	16.58	17.05	Unk	N/A	Unk	Unk	Unk
Target Mach Number	0.6	1	1	1.5	N/A	Unk	Unk	Unk
Target Dynamic Pressure	150	5985.03	5985.03	374	N/A	Unk	Unk	Unk
Actual Mach Number	0.54	0.92	0.941	0.8	N/A	Unk	Unk	Unk
Actual Dynamic Pressure	148	5999.39	5975.46	400	N/A	Unk	3000	Unk
Sources	Source 12 (Mitcheltree et al.)	Source 16 (Rodier et al.), Source 5 (Givens et al.), & Source 11 (Meltzer et al.)	Source 10 (McMenamin et al.)	Source 9 (Jakel et al.)	Source 4 (Gaborit et al.) & Source 3 (Fulchignoni et al.)	Source 18 (Witkowski et al.)	Source 7 (Hinada et al.) & Source 8 (Inatani et al.)	Source 7 (Hinada et al.)

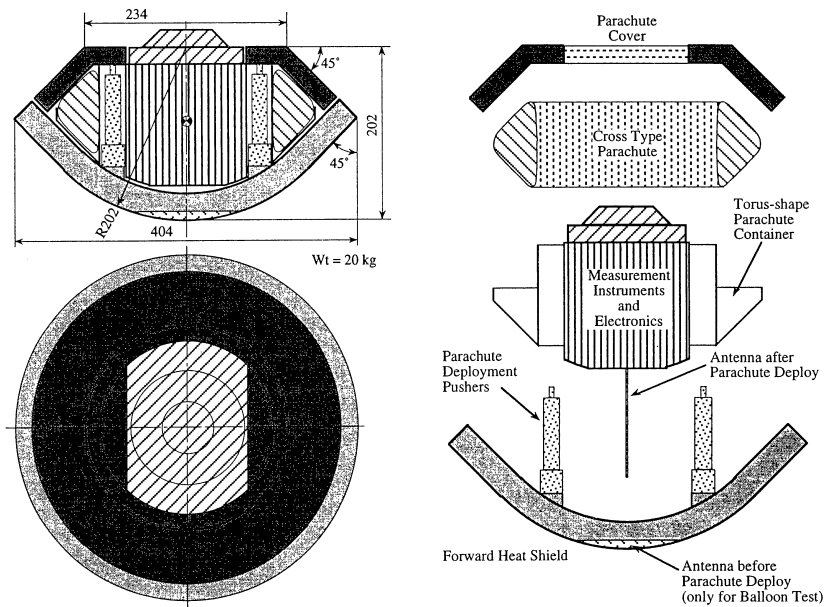


Figure 20: Hayabusa MUSES-C Drop Test Probe.⁷

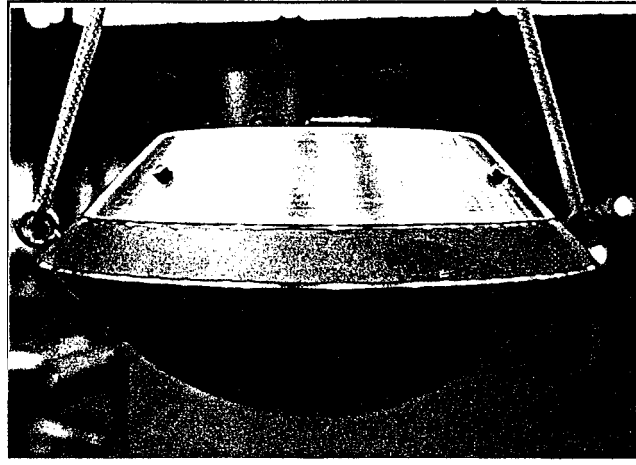


Figure 21: MUSES-C Drop Test Probe Attached to Gondola.⁹

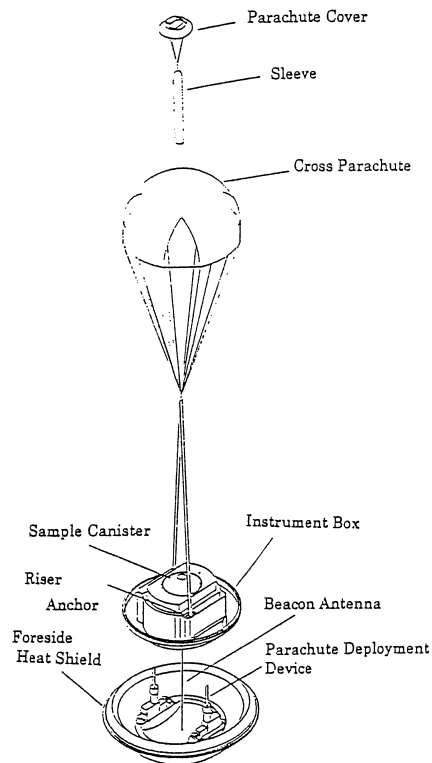


Figure 22: Hayabusa MUSES-C Parachute Deployment Sequence.⁷

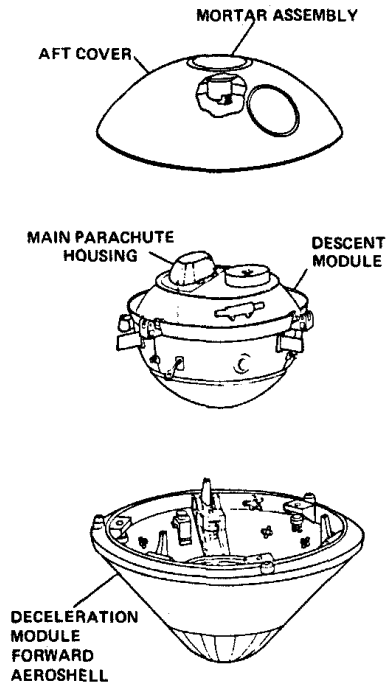


Figure 23: Galileo Probe Design.¹⁶

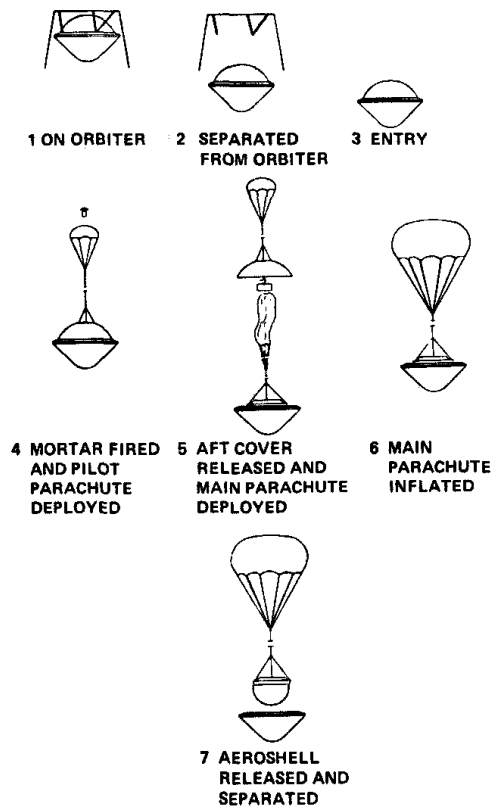


Figure 24: Galileo Parachute Deployment Sequence.¹⁶

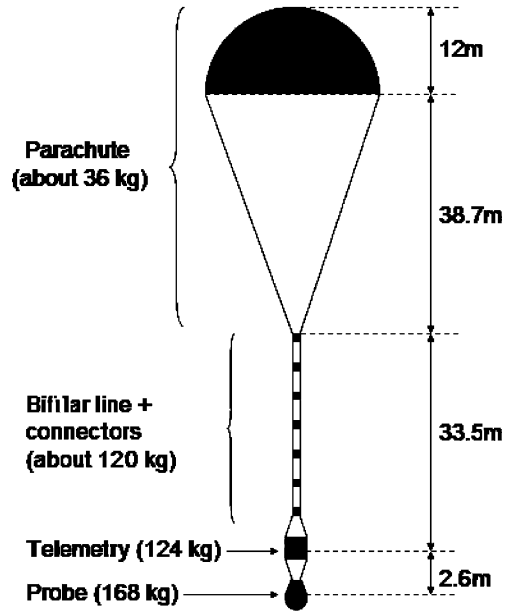


Figure 25: Huygens HASI Drop Test Descent Train.⁴



Figure 26: Huygens HASI Drop Probe (gondola, ring, cone, and upper cover).³

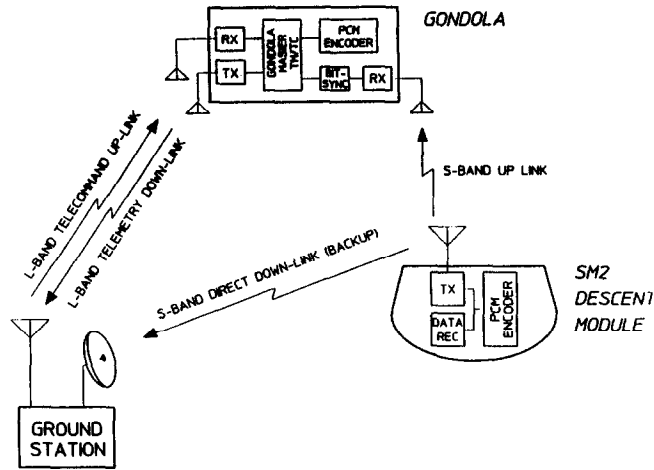


Figure 27: Huygens Systems Drop Test Data Acquisition and Telemetry Setup.⁹



Figure 28: Huygens Drop Test Probe with Gondola.⁹



Figure 29: Mars Subsonic Parachute Test Gondola with Stowed Main and Drogue Chutes.¹²



Figure 30: Mars Subsonic Parachute Testing, Pre-Launch Setup.¹²

Acknowledgments

The work described in this paper was conducted by the Georgia Institute of Technology in partnership with Aurora Flight Sciences Corporation under the NASA Small Business Technology Transfer (STTR) program. The author would like to thank Professor David Spencer for his invaluable guidance throughout the SPORE project development. The author would also like to thank the entire SPORE team (Nikki Bauer, Jenny Kelly, Justin McClellan (Aurora), Matt Nehrenz, and Allison Willingham) for their dedication and support of the SPORE effort.

References

- ¹Bixby, H. W., Ewing, E. G., and Knacke, T. W., *Recovery Systems Design Guide*, AFFDL-TR-78-151, 1978.
- ²*Conventional Balloon Flight Support: Balloon Flight Application Procedures User Handbook*, Columbia Scientific Balloon Facility, OF-600-10-H. 1 May 2006, pp. 1-40.
- ³Fulchignoni, M., Aboudan, A., Angrilli, F., Antonello, M., Bastianello, S., et al. (2004). "A Stratospheric Balloon Experiment to Test the Huygens Atmospheric Structure Instrument (HASI)," *Planetary and Space Science*, Vol. 52, No. 9, pp. 867-880.
- ⁴Gaborit, V., Antonello, M., and Colombatti, G., "Huygens Structure Atmospheric Instrument 2002 Balloon Campaign: Probe-Parachute System Attitude Analysis," *Journal of Aircraft*, Vol. 42, No. 1, Jan 2005, pp. 158-165.
- ⁵Givens, J. J., Nolte, L. J., Pochettino, L. R.. (1983). "Galileo Atmospheric Entry Probe System: Design, Development, and Test," *21st AIAA Aerospace Sciences Meeting*; Reno, NV; 10-13 Jan., p. 1-18.
- ⁶Hedlin, A. E., Fleming, E. L., Manson, A. H., et al. (1996). "Empirical Wind Model for the Upper, Middle, and Lower Atmosphere," *Journal of Atmospheric and Terrestrial Physics*, Vol. 58, No. 13, pp. 1421-1447.
- ⁷Hinada, M., Ishii, N., Hiraki, K., & Inatani, Y. (1999). "Recovery System of MUSES-C Reentry Capsule," *ESA Symposium on European Rocket and Balloon Programmes and Related Research*, 14th, Potsdam, Germany; May 31-June 3 1999, 89.
- ⁸Inatani, Y., Ishii, N., Hiraki, K., Hinada, M., Nakajima, T., et al. (1997). "Parachute Deployment Experiment for a Small Capsule Dropped from a Balloon," *AIAA, Aerodynamic Decelerator Systems Technology Conference and Seminar, 14th*, San Francisco, CA; 3-5 June 1997, p. 3-5.
- ⁹Jakel, E., Rideau, P. R., Nugteren, P. R., Underwood, J., Faucon, P., Lebreton, J-P. (1998). "Drop Test of the Huygens Probe from a Stratospheric Balloon," *Adv. Space Res.*, Vol. 21, No. 7, pp. 1033-1039.
- ¹⁰McMenamin, H. J. and Pochettino, L. R. (1984). "Galileo Parachute System Modification Program." *8th AIAA Aerodynamic Decelerator and Balloon Technology Conference*; Hyannis, MA; 2-4 April., p. 2-11.
- ¹¹Meltzer, M., *Mission to Jupiter: A History of the Galileo Project*, 1st ed., NASA Office of External Relations: NASA History Division, Washington, DC, 2007, Chap. 2.
- ¹²Mitcheltree, R., Bruno, R., Slimko, E., Baffes, C., Konefat, E., et al. (2005). "High Altitude Test Program for a Mars Subsonic Parachute". *18th AIAA Aerodynamic Decelerator Systems Technology Conference and Seminar*; Munich; Germany; 23-26 May 2005, p. 1-11.
- ¹³Mitcheltree, R.A., Moss, J.N., Cheatwood, F.M., Greene, F.A., and Braun, R.D., "Aerodynamics of the Mars Microprobe Entry Vehicles," AIAA Paper 97-3658, *Atmospheric Flight Mechanics Conference*, New Orleans, LA, August 11-13, 1997.
- ¹⁴NSC: *Near Space Corporation*. Near Space Corporation, 2011. Web. 21 Mar. 2012. <<http://www.nsc.aero>>.
- ¹⁵Payne, J. (1967). "Balloon Development for the Planetary Entry Parachute Program (Initial Balloon Design Considerations for Planetary Entry Parachute Program)," *Its Proc., 4th Aferl Sci. Balloon Symp*, 11.
- ¹⁶Rodier, R.W., Thuss, R., Terhune, J.E., (1981). "Parachute Design for the Galileo Jupiter Entry Probe." *7th AIAA Aerodynamic Decelerator and Balloon Technology Conference*; San Diego, CA; 21-23 Oct., pp. 1-9.
- ¹⁷Vinh, N., Busemann, A., and Culp, R. D., *Hypersonic and Planetary Entry Flight Mechanics*, University of Michigan Press, 1980.
- ¹⁸Witkowski, A. (1999). "The Stardust Sample Return Capsule Parachute Recovery System," *CEAS/AIAA Aerodynamic Decelerator Systems Technology Conference, 15th*, Toulouse, France; 8-11 June 1999, pp. 308-315.